The structure of Bradyrhizobium japonicum transcription factor FixK2 unveils sites of DNA binding and oxidation

Bonnet, Mariette ; Kurz, Mareike ; Mesa, Socorro ; Briand, Christophe ; Hennecke, Hauke ; Grütter, Markus G

Abstract: FixK2 is a regulatory protein that activates a large number of genes for the anoxic and microoxic, endosymbiotic, and nitrogen-fixing life styles of the -proteobacterium Bradyrhizobium japonicum. FixK2 belongs to the cAMP receptor protein (CRP) superfamily. Although most CRP family members are coregulated by effector molecules, the activity of FixK2 is negatively controlled by oxidation of its single cysteine (Cys-183) located next to the DNA-binding domain and possibly also by proteolysis. Here, we report the three-dimensional x-ray structure of FixK2, a representative of the FixK subgroup of the CRP superfamily. Crystallization succeeded only when (i) an oxidation- and protease-insensitive protein variant (FixK2(C183S)-His6) was used in which Cys-183 was replaced with serine and the C terminus was fused with a hexahistidine tag and (ii) this protein was allowed to form a complex with a 30-mer double-stranded target DNA. The structure of the FixK2-DNA complex was solved at a resolution of 1.77 Å, at which the protein formed a homodimer. The precise protein-DNA contacts were identified, which led to an affirmation of the canonical target sequence, the so-called FixK2 box. The C terminus is surface-exposed, which might explain its sensitivity to specific cleavage and degradation. The oxidation-sensitive Cys-183 is also surface-exposed and in close proximity to DNA. Therefore, we propose a mechanism whereby the oxo acids generated after oxidation of the cysteine thiol cause an electrostatic repulsion, thus preventing specific DNA binding.

DOI: https://doi.org/10.1074/jbc.M113.465484

Structure of *Bradyrhizobium japonicum* transcription factor $FixK_2$ unveils sites of DNA binding and oxidation*

Mariette Bonnet[$,1,a], Mareike Kurz[$,2] Socorro Mesa[1,b], Christophe Briand[2], Hauke Hennecke[1], Markus G. Grütter[2,*]

[1]From the ETH, Institute of Microbiology, CH-8093 Zürich, Switzerland

[2]Department of Biochemistry, University of Zürich, CH-8057 Zürich, Switzerland

[$]**These authors contributed equally**

[*]Running title: *Structure of Regulator $FixK_2$ in Complex with DNA*

[*]To whom correspondence should be addressed: Markus G. Grütter, Department of Biochemistry, University of Zürich, Winterthurerstrasse 190, CH-8057 Zürich, Switzerland. Tel.: +41-44-6355580; Fax: +41-44-6356834; E-mail: gruetter@bioc.uzh.ch

Keywords: CRP/FNR superfamily; DNA-protein interaction; gene activation; oxidative control; X-ray crystallography

---

Background: Many symbiotic nitrogen fixation genes are regulated by FixK-like proteins.
Results: The high-resolution structure of a rhizobial FixK-DNA complex was solved.
Conclusion: The structure explains how oxidation of a surface-exposed cysteine near the DNA-binding site interferes with transcription activation.
Significance: Post-translational modification of a transcription regulator by reactive oxygen species is a means to shut off gene expression.

SUMMARY

$FixK_2$ is a regulatory protein that activates a large number of genes for the anoxic and microoxic, endosymbiotic and nitrogen-fixing life styles of the α-proteobacterium *Bradyrhizobium japonicum*. $FixK_2$ belongs to the cyclic AMP receptor protein (CRP) superfamily. While most CRP-family members are co-regulated by effector molecules, the activity of $FixK_2$ is negatively controlled by oxidation of its single cysteine (C183) located next to the DNA binding domain, and possibly also by proteolysis. Here we report the three-dimensional X-ray structure of $FixK_2$, a representative of the FixK subgroup of the CRP superfamily. Crystallization succeeded only (i) when an oxidation- and protease-insensitive protein variant (C183S-$FixK_2His_6$) was used, in which C183 was replaced by serine and the C-terminus fused with a hexa-histidine tag, and (ii) when this protein was allowed to form a complex with a 30mer double-strand target DNA. The structure of the $FixK_2$-DNA complex was solved at a resolution of 1.77 Å in which the protein formed a homodimer. The precise protein-DNA contacts were identified which led to an affirmation of the canonical target sequence, the so-called $FixK_2$ box. The C-terminus is surface-exposed which might explain its sensitivity to specific cleavage and degradation. The oxidation-sensitive C183 is also surface-exposed and in close proximity to DNA. Therefore, we propose a mechanism whereby the oxo-acids generated after oxidation of the cysteine thiol cause an electrostatic repulsion, thus preventing specific DNA binding.

The CRP/FNR[3] superfamily of transcription factors comprises an important group of regulatory proteins that are widely distributed within bacteria. The name-giving proteins of this family are: the cyclic AMP receptor protein (CRP; 1) and the fumarate and nitrate reductase regulator (FNR; 2). Members of this superfamily disparately respond to a broad range of metabolic and environmental cues, thereby regulating a huge number of genes involved in vital functions such as carbon substrate utilization, virulence, nitrogen fixation,

photosynthesis, and various modes of respiratory electron transport (3). Most of the CRP/FNR-type regulators function as transcription activators, few as repressors, and their regulatory activity is generally modulated by the binding of effector molecules (*i.e.*, cofactors, prosthetic groups; 3).

Despite a remarkably low sequence identity (<25%) among the family members, the proteins are predicted to be structurally similar to the CRP protein. They all share an N-terminally located effector binding domain, an anti-parallel β-barrel that makes contact with the RNA polymerase, a long α helix that enables dimerization, and a C-terminally positioned DNA-binding domain with a helix-turn-helix (HTH) motif. Being active as homodimers, the proteins bind to a 2-fold symmetric consensus nucleotide sequence on target DNA at distinct distances upstream of the promoters of regulated genes (1–5).

Based on the primary structures of the DNA-binding and effector-binding domains, the CRP/FNR members have been classified into 21 subgroups (3). Up to now, the following eight proteins, representing seven subgroups, have been crystallized and structurally characterized (PDB numbers in parentheses): CRP (3HIF; 6), CLP (3IWZ; 7), DNR (3DKW; 8), CooA (1FT9; 9), CprK (3E6C; 10), PrfA (2BE0; 11), NtcA (3LA2; 12), and SdrP (2ZCW; 13). However, no structures are known for proteins belonging to other important subgroups such as FNR, FixK, FnrN, and NnrR. A recent structural comparison of proteins in the on- and the off-states (6, 10, 12, 14, 15) have allowed a better understanding of the allosteric mechanism triggered by the binding of cofactors, and have suggested that the cofactor-induced activation mechanism is different within each subgroup.

The *Bradyrhizobium japonicum* $FixK_2$ protein (16, 17) is a key regulator for the control of >200 genes required for microoxic, anoxic, and symbiotic growth. In root-nodule symbiosis with soybean the bacterium fixes molecular nitrogen. $FixK_2$ belongs to the FixK subgroup of the CRP/FNR superfamily but – as opposed to other superfamily members – evidence for the involvement of a co-regulator in modulating the transcription-activating activity is missing. The $FixK_2$ amino acid sequence lacks a predicted binding site for a cofactor, and more importantly, purified protein from aerobically grown $FixK_2$-overproducing *Escherichia coli* cells is active as a homodimer in an *in vitro* transcription (IVT) activation assay without a recognizable co-activator (18). Yet, $FixK_2$ activity is influenced, but in a different way. Due to unique cysteine at position 183 near the HTH motif of the DNA-binding domain, $FixK_2$ is oxidation-sensitive. Oxidation of this cysteine *in vitro* triggers the formation of a reversible intermolecular disulfide bridge between two monomers. *In vivo*, however, the more likely oxidation mechanism is the conversion of the cysteine thiol into a sulfenic, sulfinic or sulfonic acid which inactivates the protein (19). The relevance of $FixK_2$ oxidation *in vivo* is based on indirect evidence. In particular, microarray analysis had shown that most of the direct, $FixK_2$-activatable target genes displayed a decreased expression in hydrogen peroxide-stressed *B. japonicum* wild-type cells, but not in a strain having a $FixK_2$ variant with a replacement of cysteine 183 by an alanine (19). $FixK_2$ oxidation might be relevant for instantly shutting off its activity in response to reactive oxygen species (ROS) *in vivo*. ROS are produced (i) in the early stage of root-hair infection, (ii) in the process of endosymbiotic respiration, and (iii) late during nodule senescence (20-22). In all of these conditions $FixK_2$ activity might either not be necessary or not desirable. Apart from this oxidative, post-translational control $FixK_2$ is also subject to proteolysis. We have recently shown that $FixK_2$ is degraded by the housekeeping chaperone protease $ClpAP_1$ and that the preferential protease-sensitive site is located at the carboxy-terminus (23).

It was therefore of interest to crystallize $FixK_2$ and to determine its structure by X-ray crystallography. We hoped that this would help us understand how the oxidation of cysteine 183 interferes with $FixK_2$ activity and why the C-terminus is prone to proteolysis. Moreover, as it turned out that crystals were formed only when $FixK_2$ was complexed with DNA, the structure also uncovered the precise protein-DNA contact sites.

EXPERIMENTAL PROCEDURES

Plasmid construction. The QuikChange site-directed mutagenesis method (Stratagene, Basel, Switzerland) was used to exchange the codon for cysteine 183 against a serine codon, using the complementary oligonucleotides (5'-GATGGCGCTGCCGATGTCCCGCCGCGAT

ATCGGCG-3' and 3'-CGCCGATATCGCGGCGGGACATCGGCAG CGCCATC-5' (serine codons underlined) and pRJ9058 (18) as template, which yielded plasmid pRJ8848. To construct the plasmid coding for the N-terminally fused, His_6-tagged C183S-$FixK_2$, the *fixK*$_2$-containing DNA fragment was cut out with NdeI and NotI restriction enzymes and cloned in frame with the His_6-tag DNA into pET28b(+) (Novagen, Nottingham, UK), yielding plasmid pRJ8850. To obtain C-terminally fused, His_6-tagged C183S-$FixK_2$, the *fixK*$_2$ gene was first amplified by PCR from pRJ8848 with appropriate primers (forward: 5'-GCGCATATGCTGACCCAGACAC-3'; reverse: 5'-CGGCGGCCGCGGCGTCGAGATTGTGCAG GC-3') which contained sequences for the NdeI and NotI restriction sites (underlined). The PCR-amplified DNA was then cloned in the pGEM-T easy vector (Promega, Madison, USA), cut out with the aforementioned enzymes, and cloned in frame with the His_6-tag DNA into pET24c(+) (Novagen), yielding the consecutive plasmids pRJ0003 and pRJ0004. All fusion constructs were confirmed by sequencing.

Protein expression and purification. C183S-His_6FixK_2 and C183S-$FixK_2His_6$ proteins, carrying the N- and C-terminal His_6-tags, respectively, were expressed and purified as described previously (18), unless specified otherwise (see crystallization part). Selenomethionine-labeled C183S-$FixK_2His_6$ (SeMet C183S-$FixK_2His_6$) was generated using the methionine auxotrophic *E. coli* B834 (DE3) strain (Novagen). The recombinant strain was grown in SelenoMet^{TM} medium (Molecular Dimensions Ltd., Newmarket, UK) at 30°C for three hours. SeMet C183S-$FixK_2His_6$ was purified like the unlabeled protein. SeMet had replaced all eight methionines as confirmed by mass-spectrometric analysis.

In vitro transcription activation assays. Multiple-round IVT activation was carried out at 37°C as previously described (18). Briefly, 0.1 to 1 µM of C183S-$FixK_2His_6$ in modified IVT buffer (40 mM Tris-HCl, pH 7, 150 mM KCl, 0.1 mM ethylenediaminetetraacetic acid) plus the four nucleotide triphosphates was incubated in the presence of 50 nM *B. japonicum* RNA polymerase (holoenzyme) and 20 nM of template plasmid pRJ8816 at 37°C for 30 min. This plasmid harbors the *fixN* promoter region and a small part of the *fixN* gene upstream of a *B. japonicum* transcription terminator from the *rrn* operon. The electrophoretically separated transcripts were analyzed by using a PhosphorImager SF (Molecular Dynamics–GE Healthcare, Sunnyvale, USA), and signal intensities were determined with the Bio-Rad Quantity One software (Bio-Rad, Reinach, Switzerland).

Crystallization. Unlabeled, native and SeMet-labeled C183S-$FixK_2His_6$ were crystallized in the presence of 30mer double-strand target DNA from the $FixK_2$ binding site of the *fixN* promoter (sequence: CCACCTATCTTGATTTCAATCAATTCCCC G; two binding half-sites underlined). This *fixN* oligonucleotide (1 µM scale; Microsynth, Balgach, Switzerland) was prepared by heating equimolar amounts of complementary single-strand DNAs at 98°C for 5 min and slowly cooling the mixture down to room temperature afterwards. The proteins (9 mg/ml) that had been purified by immobilized metal ion affinity chromatography were mixed with 1.5-fold molar excess of *fixN* double-strand DNA and incubated for 5 min on ice. The formed DNA-protein complex was then subjected to size-exclusion chromatography on a Superdex 200 10/300 HR column (GE Healthcare) with modified IVT buffer as the running buffer and concentrated using a microcon membrane (Amicon–Merck Millipore, Billerica, USA) with a molecular-mass cutoff of 10 kDa.

Crystals of both the native and the SeMet-labeled $FixK_2$ derivatives complexed with DNA (185 mg complex/ml) were grown at 277°K by sitting-drop vapor diffusion in 0.1 M BisTris, pH 6, 0.1 M NH_4-acetate, 16-22% polyethyleneglycol (PEG) 10,000 for a period of two to four days. The complex crystallized as a protein dimer bound to DNA, and the crystals were thin and plate-like (Fig. 1).

Data collection and structure determination. Crystals were flash-frozen in liquid propane after sequential soaking in mother liquor containing 5–20% PEG400. Diffraction data were collected at 90°K at the Swiss Light Source X06SA beamline (Paul Scherrer Institute, Villigen, Switzerland) using a PILATUS 6M detector (Dectris, Baden, Switzerland) at a wavelength of 1 Å (native protein) and 0.997 Å (SeMet derivative). The $FixK_2$ structure was solved by SAD using the SeMet-labelled protein.

Data for the native and SeMet proteins were processed by using software package XDS (24). The SeMet positions were located by using the program suite SHELX (25) and the phased electron-density map was used for automatic model building with AutoSol/AutoBuild using PHENIX (26). Manual model building was performed using COOT (27), and the structure was refined first with PHENIX and then with REFMAC5 from CCP4i (28), including TLS refinement. The structure of C183S-$FixK_2His_6$ includes amino acids 38 to 232 (both monomers) of the mature 232-amino-acid protein, with one $FixK_2$ dimer in the asymmetric unit. No density was observed for the N-terminal residues 1–37 in either monomer. The four additional C-terminal residues are part of the linker region between protein and the hexa-His affinity tag, which itself is not visible in the structure. 25 and 24 of the 30 basepairs of the bound, double-strand *fixN* promoter DNA were structurally assigned (strands W and X, respectively). The nucleotides at both ends that could not be assigned will be addressed below (*i.e.*, two at the 5' end and three at the 3' end of strand W; two at the 3' end and four at the 5' end on strand X). MolProbity (http://molprobity.biochem.duke.edu) was used to assess the quality of the crystal structure. The data collection and refinement statistics are presented in Table 1. Structural figures were generated using PyMOL (Warren L. DeLano, The PyMOL Molecular Graphics System, http://www.pymol.org). Secondary Structure Matching (SSM), implemented in COOT, was used to compare the $FixK_2$ structure with other structures of the protein superfamily.

Accession Number. Coordinates and structure factors have been deposited in the Protein Data Bank with accession number 4I2O.

RESULTS AND DISCUSSION

Problem solving and crystallization of $FixK_2$. Two major obstacles stood in the way towards crystallization of $FixK_2$: the oxidation sensitivity of the protein and its sensitivity to proteolysis. Initially, an N-terminally His_6-tagged wild-type $FixK_2$ was used that failed to produce crystals. Static light-scattering analyses revealed that the protein solution was highly poly-disperse (data not shown), likely reflecting the monomer-dimer equilibrium of $FixK_2$ (18) and the different oxidation states at cysteine 183 (19). To avoid oxidation, cysteine 183 was exchanged to serine resulting in the N-terminally His_6-tagged C183S-His_6FixK_2 construct. This protein variant was active in an IVT activation assay and resistant to oxidation (data not shown), but did not crystallize either. Furthermore, C183S-His_6FixK_2 co-purified with a truncated form, which was identified by mass spectrometry as a 220-amino-acid derivative lacking twelve amino acids from the C-terminus (named C183S-His_6FixK_2-220) (Fig. 2a). Although this cleaved variant remained soluble, it was inactive in the IVT activation test (data not shown). Exchange of the amino acids valine 220 and leucine 221 before and after the cleavage site against asparagine or threonine did not abolish cleavage. Cleavage was prevented, however, by using a C-terminally His_6-tagged $FixK_2$ variant (C183S-$FixK_2His_6$). This variant was purified with high yield as an apparently homogeneous, full-length protein (Fig. 2a; molecular mass 26,883 Da). Despite the relative proximity of the His_6-tag to the DNA-binding domain, the C183S-$FixK_2His_6$ variant was active in the IVT activation assay (Fig. 2b), and was successfully used in subsequent crystallization trials.

As of today, three structures of proteins from the CRP/FNR family are available in their cofactor-free apo-form (6, 10, 12). The majority of the structures available are in complex with their cognate cofactor, and only two structures have the target DNA bound (10, 29). As no cofactor has been identified so far for $FixK_2$, we attempted to crystallize C183S-$FixK_2His_6$ in the absence or presence of a 30mer double-strand target DNA harboring the $FixK_2$ binding site from the promoter of the *fixNOQP* operon (17). Numerous crystallization conditions and methods, protein concentrations and temperatures were varied over a broad range, resulting finally in a condition that yielded crystals of C183S-$FixK_2His_6$ in complex with DNA. The initial crystals diffracted highly anisotropically to a resolution of about 3 Å. Fine-slicing around the pH of the original condition, and optimizing the cryo-conditions for plunge-freezing resulted in satisfactory crystals (Fig. 1) that diffracted to a resolution <2 Å. We solved the structure of the C183S-$FixK_2His_6$-DNA complex by single wavelength anomalous dispersion (SAD) and refined it to a final resolution of 1.77 Å, with R-factor and R-free values of 18.3% and 22.7%, respectively (Table 1 and Fig. 3).

Survey on structural features. The electron density map allowed an unequivocal assignment of amino acids 38 to 232 of the 232-amino-acid $FixK_2$ monomer (Fig. 3). Hence, the predicted secondary structure elements β1 and αA in the N-terminal 37-amino-acid stretch (Fig. 4) are not visible in the structure. All other secondary structure elements displayed in Fig. 4 have been confirmed by the crystal structure. With the N-terminal region included, each monomer in the dimeric $FixK_2$ protein contains seven alpha-helices (αA to αG) and twelve beta-sheets (β1 to β12) (Fig. 4). The full-length protein comprises two major domains, (i) the N-terminal half (residues 1–127: αA–αB, and β1–β9) containing the double-stranded β-roll structure (residues 41–116: β2–β9), which in other CRP/FNR family members corresponds to the effector-binding domain, and (ii) the C-terminal DNA-binding domain (residues 155–236: αD–αG, and β10–β12) with the winged helix-turn-helix fold (residues 184–216: αE and αF). The two major domains are connected by the long α-helix (residues 128–154: αC), which is involved in dimerization of the two monomers. The dimeric C183S-$FixK_2His_6$ structure displays a perfect twofold symmetry (Fig. 3). For the DNA molecule, electron density could be seen and bases assigned for 25 out 30 (strand W), and 24 out of 30 nucleotides (strand X). Due to its nearly perfect palindromic sequence, which is interrupted by four nucleotides (TTGAT–N_4–ATCAA; inverted repeat underlined) the bound DNA molecule displays a quasi-twofold symmetry.

The overall architecture of the DNA-protein complex with $FixK_2$ is largely similar to that of CRP and CprK (Fig. 5). Nevertheless the structures do not superimpose ideally, giving relatively high root mean square deviations (r.m.s.d.) of 2.08 Å (for 175 C_α atoms) and 3.27 Å (for 177 C_α atoms) for CRP and CprK, respectively. These deviations can primarily be explained by the different arrangement of the DNA portion in the complexes as well as by differences in the C-terminal parts of the proteins.

The overall surface of the $FixK_2$ protein appears to exhibit an equal distribution of hydrophobic and hydrophilic patches. A notable surface feature of $FixK_2$ is the presence of one negatively charged cavity per monomer (Fig. 6). Superimposition with CRP showed that this area corresponds to the hydrophobic cAMP-binding pocket in the CRP effector-binding domain. The amino acid residues forming the pockets are not conserved between CRP and $FixK_2$. Although $FixK_2$, in comparison with CRP, must be present in a higher protein concentration to be active in an IVT activation assay, it does not require the addition of a co-activating compound such as cAMP in the case of CRP. Previous work has shown that neither cAMP nor cGMP alters the concentration-dependent elution behavior of $FixK_2$ during size-exclusion chromatography (18). Whether or not the aforementioned negatively charged cavity of $FixK_2$ functions in the binding of a yet unidentified cofactor remains an open question. SdrP, another CRP/FNR family member, has also been shown to be active *in vitro* without any cofactor. SdrP crystallizes in an active form without DNA bound. Contrary to $FixK_2$, however, its crystal structure clearly lacks the putative cofactor binding pocket (13) because bulky amino acid residues fill the corresponding positions where cAMP occupies the pocket in CRP.

Surface-exposed C-terminus, a possible target for degradation. As reported above, the N-terminally His_6-tagged C183S-$FixK_2$ derivative suffered a truncation during the purification procedure through specific proteolytic cleavage at the C-terminus between valine 220 and leucine 221. Moreover, recent work showed that the C-terminus in $FixK_2$ is a recognition site for the $ClpAP_1$ chaperone protease leading to complete degradation of the protein (23). Hence, the C-terminus appears to be a critical determinant for protease sensitivity.

The structure of our $FixK_2$-DNA complex now showed that the C-terminal helix (αG) is clearly surface-exposed, rendering the protein susceptible to specific cleavage and $ClpAP_1$-mediated recognition (Fig. 7). Cleavage between valine 220 and leucine 221 disrupts the carboxy-end of beta-strand β12 (Fig. 4). Interestingly, β12 is the intermediate β-strand of a small β-sheet formed by β10, β11, and β12 near the DNA-binding domain. Although this β-sheet does not directly interact with the bound DNA (Fig. 7), hydrogen bonds are formed between β12 and αG, and between αG and αE of the HTH-motif. Therefore, disrupting these hydrogen bonds by proteolytic removal of the last twelve amino acids might affect the DNA-binding domain, leading to inactivation of the protein. In fact, this assumption was confirmed by DNA-band shift assays, in which the

truncated C183S-His_6FixK_2-220 variant was found to be unable to bind DNA (data not shown), which explains its inactivity in the IVT activation assay (see above).

The C-terminal helix (αG) is also present in some other members of the CRP/FNR superfamily (CprK, 10; PrfA, 11; SdrP, 13) and therein plays a crucial role in DNA-binding and activity. In CprK, for example, the C-terminus interacts directly with DNA in the on-state, but is unstructured in the apo-form (10), and in PrfA, the C-terminus stabilizes the DNA binding domain (11). For the latter, mutations of the last helices were found to abolish DNA-binding, rendering PrfA inactive (30).

Characteristics of protein-DNA interactions. As stated before, only two other structures of the homologues CRP (29) and CprK (10) have been solved in complex with their cognate DNA. The crystallization of C183-$FixK_2His_6$ in complex with a cognate target DNA allowed us to gain detailed insight into the interactions between amino acids of the HTH-motif and nucleotides of the so-called $FixK_2$ box, a specific and conserved DNA sequence in the promoter region of at least 20 *bona fide* $FixK_2$-activated genes (18, 19). The $FixK_2$ box consists of 14 bases that include the minimal consensus sequence TTG–N_8–CAA. Mutations in the $FixK_2$ box abolish activation of transcription by $FixK_2$ (18). The structure revealed that three amino acids in helix αF (L195, E196, R200) of the HTH motif directly interact with bases of the $FixK_2$ box (Fig. 8). L195 of either monomer forms a hydrophobic interaction with base T8 (strand W) and T8' (strand X). E196 of either monomer forms a hydrogen bond with C19 (strand W) and C19' on strand X (Fig. 8). Interestingly, the guanidinium moiety of arginine 200 interacts strongly by complex hydrogen bonding with two bases located on different strands of the DNA molecule. Bidentate interactions are formed with G10/G10', and one additional hydrogen bond with T18'/T18 (monomers A/B) (Fig. 8 and Fig. 9). These specific interactions between bases and amino acids are the hallmark of $FixK_2$-DNA binding. Applying bioinformatics analysis, Dufour and co-workers (31) predicted that the conserved protein sequence (I/L/V)EXXXR applies as a DNA-binding motif for the entire FixK subgroup of all α-proteobacteria. Here, we can perfectly validate this hypothesis, since the $FixK_2$ binding motif reads $L_{195}E_{196}XXXR_{200}$ (Fig. 4). The R200-interacting T18 and T18' bases are located immediately adjacent to the core consensus sequence TTG–N_8–CAA of the previously defined $FixK_2$ box, *i.e.*, they come to lie within the more variable region (N_8). Hence, a fourth nucleotide must be considered as being part of the $FixK_2$-interacting DNA, such as TTGA-N_6-$T^{(18)}$CAA on strand W. To maintain a strong interaction with the $FixK_2$ box, the base at position 18 may alternatively be a G, a requirement imposed by the restricted hydrogen bonding of an arginine side chain to either a T or a G (32). We therefore postulate a refined consensus sequence for the $FixK_2$ box, TTG(A/C)–N_6–(T/G)CAA, which coincides reasonably well with the consensus sequence deduced from an alignment of approved $FixK_2$ box-associated promoter sequences (16).

A similar complex DNA-protein interaction network can be found for CRP. As in $FixK_2$, in CRP the second helix of the HTH motif penetrates the major groove of the DNA, and three conserved specific amino acid side chains (R180, E181, R185) interact directly via hydrogen bonds with DNA-bases, forming a REXXXR motif. These specific residues perfectly superimpose with the LEXXXR binding sequence in $FixK_2$. Despite a similar primary recognition pattern the DNA in the $FixK_2$ complex structure is less bent, approximately 55°. In contrast, the observed DNA bend in the CRP complex structure is 90° (PDB 1J59; 14). As in the CRP structure, the DNA bend in the $FixK_2$ structure contains two sharp primary kinks between the pseudo symmetry-related nucleotide pairs W T9 and W G10, and W C19 and W A20. Two secondary kinks are also formed: W G3 and W G4, and W A25 and W G26. In general, the required energy to bend the DNA is compensated by the very specific interactions as described above and between protein side chains and the DNA phosphates. Several indirect protein-DNA interactions were also observed (Fig. 8). These are located in the short loop between the dimerization helix αC and helix αD, as well as in the HTH-motif and nearby. The interactions occur through side chain residues and the DNA-phosphate backbone or via water molecules, and in a few cases via the amino acid peptide bond and the DNA phosphodiester bond (Fig. 8). These additional interactions, especially the hydrogen bonds located in the inter-αC–αD loop, might contribute to positioning the HTH-motif in an appropriate conformation for DNA

binding. It has been observed in other CRP/FNR-family proteins (CRP, CprK, NtcA) that the position of αF in the HTH-motif and, hence, its orientation towards the major groove of DNA may change after co-factor binding, which in these proteins is a pre-requisite for the association with DNA (10, 12, 15, 29, 33). Although CRP and $FixK_2$ exhibit a similar number of hydrogen-bond and ionic interactions between the protein side chains and the DNA phosphates, the ones in CRP are more frequently near the secondary kink, which might explain the stronger bending of bound DNA.

The critical role of cysteine 183 in the oxidative control of the $FixK_2$ protein. One of the regulatory complexes for low-oxygen sensing and signal transduction in *B. japonicum* is a two-component regulatory system, FixLJ, which controls the activation of the *$fixK_2$* gene (17). Once expressed, the $FixK_2$ protein then activates the expression of a large number of genes for microoxic and anoxic energy metabolism (17). Such a sequentially operating cascade of positive controls asks for a negative control that keeps gene expression balanced according to needs. We have previously discovered that ROS negatively interfere with $FixK_2$ by inhibiting its activity through oxidation of the single cysteine at position 183 in the protein (19). Here, we were interested to see if the structure of the $FixK_2$-DNA complex could explain how oxidation of C183 blocks activity.

In the crystallized C183S-$FixK_2$ variant the serine hydroxyl replaces the oxidation-sensitive cysteine thiol. As shown in Fig. 10, the S183 is clearly surface-exposed. It is therefore conceivable that C183 in the equivalent position of the wild-type protein is readily accessible for oxidation. In monomer A of the C183S-$FixK_2$ structure, the side-chain oxygen of S183 is 4.5 Å away from the phosphodiester between nucleotides A6 and A7 (Fig. 11), which corresponds to the T6'–C7' phosphate backbone near monomer B. Given that the Van der Waals radius of sulfur (r_w = 1.8 Å) is larger than that of the oxygen in S183 (r_w = 1.52 Å), the C183 thiol is predicted to be even closer to the DNA phosphate backbone. Thereby, C183 might partially fill the space between protein and DNA, yet allowing sufficient distance to the phosphate backbone of DNA.

Upon ROS-mediated oxidation, the conversion of the C183 thiol into sulfinic ($–SO_2^-$) or sulfonic acid derivatives ($–SO_3^-$) has serious consequences. As a corollary of thiol oxidation, the more bulky, negatively charged sulfoxides will not only cause a steric hindrance of the protein-DNA interaction but also an electrostatic repulsion of the opposite, negatively charged DNA phosphate, preventing $FixK_2$ binding to DNA or at least DNA bending. However, we cannot completely exclude that such a chemical modification might contribute to a conformational change of the DNA-binding domain, thus resulting in a loss of target DNA recognition.

Previous work has shown that strong over-oxidation of $FixK_2$ also affects methionines, which become oxidized to methionine sulfoxides. It was not known, however, how many and which of the eight methionines in each $FixK_2$ monomer had been targeted (19). The structure now shows that only methionine 177 is surface-exposed (Fig. 10), which makes it a prime candidate for oxidation besides C183. However, since M177 is 10 Å away from the nearest DNA phosphate backbone, its irreversible oxidation might not obstruct DNA binding directly. This is corroborated by the fact that treatment of a C183A-$FixK_2$ variant with 0.1 mM hydrogen peroxide, a condition that leads to protein methionine oxidation, did not inhibit the transcription-activating activity of $FixK_2$ (19). Thus, C183 is undoubtedly the most sensitive target, whose oxidation renders $FixK_2$ inactive.

In conclusion, the surface exposure of the single cysteine 183 and the proximity of the side-chain thiol to DNA, when $FixK_2$ is bound to the $FixK_2$-box, are the two key features that explain why ROS inhibits this transcription factor post-translationally. Oxidation-sensitive cysteine thiols have also been described for the *Desulfitobacterium dehalogenans* CprK protein, but these form either intra- or inter-subunit disulfide bridges upon oxidation (10). Interestingly, inhibition of a regulatory protein via one cysteine (C179) has recently been described for the *B. japonicum* OsrA protein, which is an anti-sigma factor of the EcfF sigma factor (34). To the best of our knowledge, our investigation on $FixK_2$ is the first known example for a member of the CRP/FNR superfamily where this kind of modification has found a structural explanation.

REFERENCES

1. Busby, S., and Ebright, R. H. (1999) Transcription activation by catabolite activator protein (CAP). *J. Mol. Biol.* **293**, 199–213
2. Kiley, P. J., and Beinert, H. (1998) Oxygen sensing by the global regulator, FNR: the role of the iron-sulfur cluster. *FEMS Microbiol. Rev.* **22**, 341–352
3. Körner, H., Sofia, H. J., and Zumft, W. G. (2003) Phylogeny of the bacterial superfamily of Crp-Fnr transcription regulators: exploiting the metabolic spectrum by controlling alternative gene programs. *FEMS Microbiol. Rev.* **27**, 559–592
4. Lawson, C. L., Swigon, D., Murakami, K. S., Darst, S. A., Berman, H. M., and Ebright, R. H. (2004) Catabolite activator protein: DNA binding and transcription activation. *Curr. Opin. Struct. Biol.* **14**, 10–20
5. Fic, E., Bonarek, P., Gorecki, A., Kedracka-Krok, S., Mikolajczak, J., Polit, A., Tworzydlo, M., Dziedzicka-Wasylewska, M., and Wasylewski, Z. (2009) cAMP receptor protein from *Escherichia coli* as a model of signal transduction in proteins – a review. *J. Mol. Microbiol. Biotechnol.* **17**, 1–11
6. Sharma, H., Yu, S., Kong, J., Wang, J., and Steitz, T. A. (2009) Structure of apo-CAP reveals that large conformational changes are necessary for DNA binding. *Proc. Natl. Acad. Sci. U.S.A* **106**, 16604–16609
7. Chin, K. H., Lee, Y. C., Tu, Z. L., Chen, C. H., Tseng, Y. H., Yang, J. M., Ryan, R. P., McCarthy, Y., Dow, J. M., Wang, A. H., and Chou, S. H. (2010) The cAMP receptor-like protein CLP is a novel c-di-GMP receptor linking cell-cell signaling to virulence gene expression in *Xanthomonas campestris*. *J. Mol. Biol.* **396**, 646–662
8. Giardina, G., Castiglione, N., Caruso, M., Cutruzzola, F., and Rinaldo, S. (2011) The *Pseudomonas aeruginosa* DNR transcription factor: light and shade of nitric oxide-sensing mechanisms. *Biochem. Soc. Transact.* **39**, 294–298
9. Lanzilotta, W. N., Schuller, D. J., Thorsteinsson, M. V., Kerby, R. L., Roberts, G. P., and Poulos, T. L. (2000) Structure of the CO sensing transcription activator CooA. *Nat. Struct. Biol.* **7**, 876–880
10. Levy, C., Pike, K., Heyes, D. J., Joyce, M. G., Gabor, K., Smidt, H., van der Oost, J., and Leys, D. (2008) Molecular basis of halorespiration control by CprK, a CRP-FNR type transcriptional regulator. *Mol. Microbiol.* **70**, 151–167
11. Eiting, M., Hageluken, G., Schubert, W. D., and Heinz, D. W. (2005) The mutation G145S in PrfA, a key virulence regulator of *Listeria monocytogenes*, increases DNA-binding affinity by stabilizing the HTH motif. *Mol. Microbiol.* **56**, 433–446
12. Zhao, M. X., Jiang, Y. L., He, Y. X., Chen, Y. F., Teng, Y. B., Chen, Y., Zhang, C. C., and Zhou, C. Z. (2010) Structural basis for the allosteric control of the global transcription factor NtcA by the nitrogen starvation signal 2-oxoglutarate. *Proc. Natl. Acad. Sci. U.S.A* **107**, 12487–12492
13. Agari, Y., Kashihara, A., Yokoyama, S., Kuramitsu, S., and Shinkai, A. (2008) Global gene expression mediated by *Thermus thermophilus* SdrP, a CRP/FNR family transcriptional regulator. *Mol. Microbiol.* **70**, 60–75
14. Parkinson, G., Wilson, C., Gunasekera, A., Ebright, Y. W., Ebright, R. H., and Berman, H. M. (1996) Structure of the CAP-DNA complex at 2.5 angstroms resolution: a complete picture of the protein-DNA interface. *J. Mol. Biol.* **260**, 395–408
15. Popovych, N., Tzeng, S. R., Tonelli, M., Ebright, R. H., and Kalodimos, C. G. (2009) Structural basis for cAMP-mediated allosteric control of the catabolite activator protein. *Proc. Natl. Acad. Sci. U.S.A* **106**, 6927–6932
16. Mesa, S., Hauser, F., Friberg, M., Malaguti, E., Fischer, H. M., and Hennecke, H. (2008) Comprehensive assessment of the regulons controlled by the FixLJ-$FixK_2$-$FixK_1$ cascade in *Bradyrhizobium japonicum*. *J. Bacteriol.* **190**, 6568–6579
17. Nellen-Anthamatten, D., Rossi, P., Preisig, O., Kullik, I., Babst, M., Fischer, H. M., and Hennecke, H. (1998) *Bradyrhizobium japonicum* $FixK_2$, a crucial distributor in the FixLJ-

dependent regulatory cascade for control of genes inducible by low oxygen levels. *J. Bacteriol.* **180**, 5251–5255
18. Mesa, S., Ucurum, Z., Hennecke, H., and Fischer, H. M. (2005) Transcription activation in vitro by the *Bradyrhizobium japonicum* regulatory protein $FixK_2$. *J. Bacteriol.* **187**, 3329–3338
19. Mesa, S., Reutimann, L., Fischer, H. M., and Hennecke, H. (2009) Posttranslational control of transcription factor $FixK_2$, a key regulator for the *Bradyrhizobium japonicum*–soybean symbiosis. *Proc. Natl. Acad. Sci. U.S.A* **106**, 21860–21865
20. Pauly, N., Pucciariello, C., Mandon, K., Innocenti, G., Jamet, A., Baudouin, E., Herouart, D., Frendo, P., and Puppo, A. (2006) Reactive oxygen and nitrogen species and glutathione: key players in the legume-*Rhizobium* symbiosis. *J. Exp. Bot.* **57**, 1769–1776
21. Chang, C., Damiani, I., Puppo, A., and Frendo, P. (2009) Redox changes during the legume-rhizobium symbiosis. *Mol. Plant* **2**, 370–377
22. Santos, R., Herouart, D., Sigaud, S., Touati, D., and Puppo, A. (2001) Oxidative burst in alfalfa–*Sinorhizobium meliloti* symbiotic interaction. *Mol. Plant-Microbe Interact.* **14**, 86–89.
23. Bonnet, M., Stegmann, M., Maglica, Z., Stiegeler, E., Weber-Ban, E., Hennecke, H., and Mesa, S. (2013) $FixK_2$, a key regulator in *Bradyrhizobium japonicum*, is a substrate for the protease ClpAP in vitro. *FEBS Lett.* **587**, 88–93
24. Kabsch, W. (2010) XDS. *Acta Crystallogr. D Biol. Crystallogr.* **66**, 125–132
25. Schneider, T. R., and Sheldrick, G. M. (2002) Substructure solution with SHELXD. *Acta Crystallogr. D Biol. Crystallogr.* **58**, 1772–1779
26. Adams, P. D., Afonine, P. V., Bunkoczi, G., Chen, V. B., Davis, I. W., Echols, N., Headd, J. J., Hung, L. W., Kapral, G. J., Grosse-Kunstleve, R. W., McCoy, A. J., Moriarty, N. W., Oeffner, R., Read, R. J., Richardson, D. C., Richardson, J. S., Terwilliger, T. C., and Zwart, P. H. (2010) PHENIX: a comprehensive Python-based system for macromolecular structure solution. *Acta Crystallogr. D Biol. Crystallogr.* **66**, 213–221
27. Emsley, P., and Cowtan, K. (2004) COOT: model-building tools for molecular graphics. *Acta Crystallogr. D Biol. Crystallogr.* **60**, 2126–2132
28. Murshudov, G. N., Vagin, A. A., and Dodson, E. J. (1997) Refinement of macromolecular structures by the maximum-likelihood method. *Acta Crystallogr. D Biol. Crystallogr.* **53**, 240–255
29. Schultz, S. C., Shields, G. C., and Steitz, T. A. (1991) Crystal structure of a CAP-DNA complex: the DNA is bent by 90 degrees. *Science* **253**, 1001–1007
30. Herler, M., Bubert, A., Goetz, M., Vega, Y., Vazquez-Boland, J. A., and Goebel, W. (2001) Positive selection of mutations leading to loss or reduction of transcriptional activity of PrfA, the central regulator of *Listeria monocytogenes* virulence. *J. Bacteriol.* **183**, 5562–5570
31. Dufour, Y. S., Kiley, P. J., and Donohue, T. J. (2010) Reconstruction of the core and extended regulons of global transcription factors. *PLoS Genet.* **6**, e1001027
32. Luscombe, N. M., Laskowski, R. A., and Thornton, J. M. (2001) Amino acid-base interactions: a three-dimensional analysis of protein-DNA interactions at an atomic level. *Nucleic Acids Res.* **29**, 2860–2874
33. Passner, J. M., and Steitz, T. A. (1997) The structure of a CAP-DNA complex having two cAMP molecules bound to each monomer. *Proc. Natl. Acad. Sci. U.S.A* **94**, 2843–2847
34. Masloboeva, N., Reutimann, L., Stiefel, P., Follador, R., Leimer, N., Hennecke, H., Mesa, S., and Fischer, H. M. (2012) Reactive oxygen species-inducible ECF sigma factors of *Bradyrhizobium japonicum*. *PloS One* **7**, e43421

Acknowledgements – All data were collected at the Swiss Light Source (SLS, Paul Scherrer Institute, Villigen, Switzerland). We thank the people of the MX group for their outstanding support at the SLS, and B. Blattmann and C. Stutz-Ducommun from the Protein Crystallization Center at the University of Zurich for their excellent laboratory support during the crystallization.

FOOTNOTES

*This work was supported by grants from the Swiss National Science Foundation to HH, SM, and MGG, and by funds from the ETH Zurich and University of Zurich. Furthermore, work in the laboratory of MGG was financially supported through the framework of the National Center of Competence in Research (NCCR) for Structural Biology. SM thanks the Ministerio de Economía y Competitividad of Spain for financial support.

[1]ETH, Institute of Microbiology, Wolfgang-Pauli-Strasse 10, CH-8093 Zürich, Switzerland.
[2]Department of Biochemistry, University of Zürich, Winterthurerstrasse 190, CH-8057 Zürich, Switzerland.
[a]Present address: Center for Interdisciplinary Research in Biology, College de France, F-75005 Paris, France.
[b]Present address: Department of Soil Microbiology and Symbiotic Systems, Estación Experimental del Zaidín, CSIC, E-18008 Granada, Spain.

[3]The abbreviations used are: CRP, cAMP receptor protein; FNR, fumarate and nitrate reductase regulator; HTH, helix-turn-helix; IVT, *in vitro* transcription; PDB, Protein Data Bank; PEG, polyethylene glycol; r.m.s.d., root mean square deviation; ROS, reactive oxygen species; SAD, single wavelength anomalous dispersion; SeMet, selenomethionine.

FIGURE LEGENDS

FIGURE 1. Crystals of the C183S-Fix$K_2$$His_6$ protein in complex with DNA. The thin and platelike crystals were grown by vapour diffusion in 0.1 M BisTris, pH 6, 0.1 M NH_4-acetate, 16-22% PEG 10,000 at 277°K within 2–4 days. The scale bar corresponds to 200 µm.

FIGURE 2. Tests for purity and activity of the C183S-Fix$K_2$$His_6$ protein. (a) Coomassie blue-stained gel after SDS-polyacrylamide gel electrophoresis of purified N-terminally and C-terminally His_6-tagged C183S-FixK_2 proteins. The N-terminally tagged construct co-purifies with a truncated version (C183S-His_6FixK_2-220) that lacks the twelve C-terminal amino acids. (b) IVT activation assay with 0.1 to 1 µM of C183S-Fix$K_2$$His_6$ added to the test mixture. Plasmid template (pRJ8816) containing the FixK_2-dependent *fixN* promoter cloned upstream of a strong transcription terminator was used for multiple-round *in vitro* transcription with RNA polymerase holoenzyme from *B. japonicum*. A FixK_2-independent transcript encoded by the plasmid served as a useful internal control for the RNA polymerase activity. The left two lanes contain RNA size markers with lengths of 180 (M) and 286 nucleotides (M').

FIGURE 3. Ribbon representation of the C183S-Fix$K_2$$His_6$ protein bound to FixK_2 box-containing target DNA. The protein-DNA complex crystallized in space group $P2_1$. The structure was solved by SAD methods and refined to 1.77 Å with R-factor and R-free values of 18.3% and 22.7%, respectively. Due to the lack of electron density at the N-terminus, the first 37 amino acids of C183S-Fix$K_2$$His_6$ could not be modelled. Likewise, few nucleotides at both ends of the 30mer DNA could not be structurally determined (see Experimental Procedures). The two monomers are shown in red and blue and some important secondary structure elements have been labelled, i.e. the dimerization helix αC, and αF from the HTH-motif harbouring the DNA-binding sequence $L_{195}E_{196}XXXR_{200}$. The figure was generated using Pymol (http://www.pymol.org).

FIGURE 4. Secondary structure of FixK_2. The secondary structure elements (determined with DSSM using the structure of C183S-Fix$K_2$$His_6$) are colored in red (α-helices) and blue (β-strands). Amino acid residues and secondary structure elements (predicted from the sequence using PSIPred) that are not seen in the solved structure due to the lack of electron density are depicted in light coloration.

Further structural elements relevant for this work are highlighted as follows: frame, HTH motif; white letters, amino acids in the LEXXXR motif of helix αF making contact with DNA at $FixK_2$ box; asterisk, oxidation-sensitive cysteine 183; underlining, the 12 amino acids that are cleaved off when the C-terminus is not protected by a His_6-tag.

FIGURE 5. Superimposition of C183S-$FixK_2His_6$ (red colour), CRP (green colour, 1J59[14]) and CprK (blue colour, 3E6C[10]). The overall architecture of the homologues protein is largely similar, displaying the same overall structural fold. However, CRP and CprK show a stronger DNA-bending (90° and 80°, respectively) than C183S-$FixK_2His_6$ (approximately 55°).

FIGURE 6. Electrostatic surface of C183S-$FixK_2His_6$. The structure is shown in two different orientations, related by a 90° rotation along the y-axis. Red indicates negatively charged regions (–12 kT) and blue positively charged regions (+12 kT). Uncharged surfaces are shown in white. The surface shows a negatively charged cavity (encircled) that superimposes well with the cAMP binding pocket of CRP. The image was generated using the APBS tool in Pymol.

FIGURE 7. Top view of the structure of C183S-$FixK_2His_6$ in complex DNA. The two monomers are shown in red and blue. The twelve C-terminal amino acids of the protein are colored in yellow. They are surface exposed, rendering the protein accessible to specific proteolytic cleavage and complete degradation. The three β-strands near the protease-sensitive site (β10 to β12) are marked on one monomer, and the entire β-sheet is encircled.

FIGURE 8. Schematic representation of information on the contact sites between $FixK_2$ protein and target DNA deduced from the high-resolution structure. Amino acids that undergo specific interactions with nucleotides are marked with boldface letters. The core $FixK_2$ box is underlined. The grey nucleotides at both ends are those that could not be modelled due to lack of electron density. The types of interactions are indicated in the lower left corner.

FIGURE 9. Selected section of the structure around arginine 200 (monomer A), showing the complex hydrogen bond interactions to two bases of opposite DNA strands, *i.e.,* G10 on strand W, and T18' on strand X.

FIGURE 10. Surface representation of C183S-$FixK_2His_6$ protein bound to DNA. The two monomers are shown in red and blue. Serine 183 is surface exposed and in close proximity to the DNA. In the wild-type protein, oxidation of C183 at this position most likely inactivates the protein through steric hindrance of DNA binding or electrostatic repulsion of the DNA. Methionine 177 is highlighted as well, being the only one out of eight methionines that is located on the surface of the protein. Met 177 is accessible to oxidation, but its oxidation does not influence protein activity.

FIGURE 11. Selected electron density map. The sector around serine 183 is shown. The final $2F_o$-F_c map is contoured at 1 σ and superimposed on the atomic model. The distance to the nearest phosphate of DNA is given.

TABLE 1
Statistics of data collection and structural refinement of native and SeMet C183S-Fix$K_2$$His_6$-DNA complex

Data collection	SeMet C183S-Fix$K_2$$His_6$ (SAD data)	Native C183S-Fix$K_2$$His_6$
Wavelength (Å)	0.97961	1.00002
Resolution range (Å)	43.97-3.00 (3.08-3.00)	43.58-1.77 (1.83-1.77)
Spacegroup	$P12_11$	$P12_11$
Cell dimensions		
a,b,c (Å)	111.48, 43.97, 69.92	111.33, 43.88, 70.11
α,β,γ (°)	90, 89.98, 90	90, 90.04, 90
Unique reflections[a]	26587 (1987)	66473 (6610)
Redundancy[a]	9.5 (9.5)	6.6 (6.8)
Completeness[a] (%)	99.9 (100)	99.7 (100)
$<I/\sigma(I)>$[a]	17.08 (4.66)	21.82 (3.8)

Refinement	
No. reflections (work set/test set)	66510/3315
R_{factor}[b]/R_{free}[c] (%)	18.30/22.71
No. of atoms	
Protein (chains A/B)	1541/1541
DNA (strands W/X)	522/478
water	496
AverageB factor (Å^2)	
Protein (chains A/B)	30.7/30.7
DNA (strands W/X)	57.2/52.7
water	40.4
Wilson B	23.76
Rmsd from ideal	
Bond lengths (Å)	0.018
Bond angles (°)	2.064
Ramachandran plot	
favored (%)	98.98
allowed regions (%)	1.02

[a]Values in parentheses refer to the outermost resolution shell. [b]$R_{factor} = \sum_h |F_o - F_c| / \sum_h |F_o|$, where F_o and F_c are the observed and calculated structure-factor amplitudes for each reflection h. [c]R_{free} was calculated for a randomly selected 10% of data omitted from refinement.

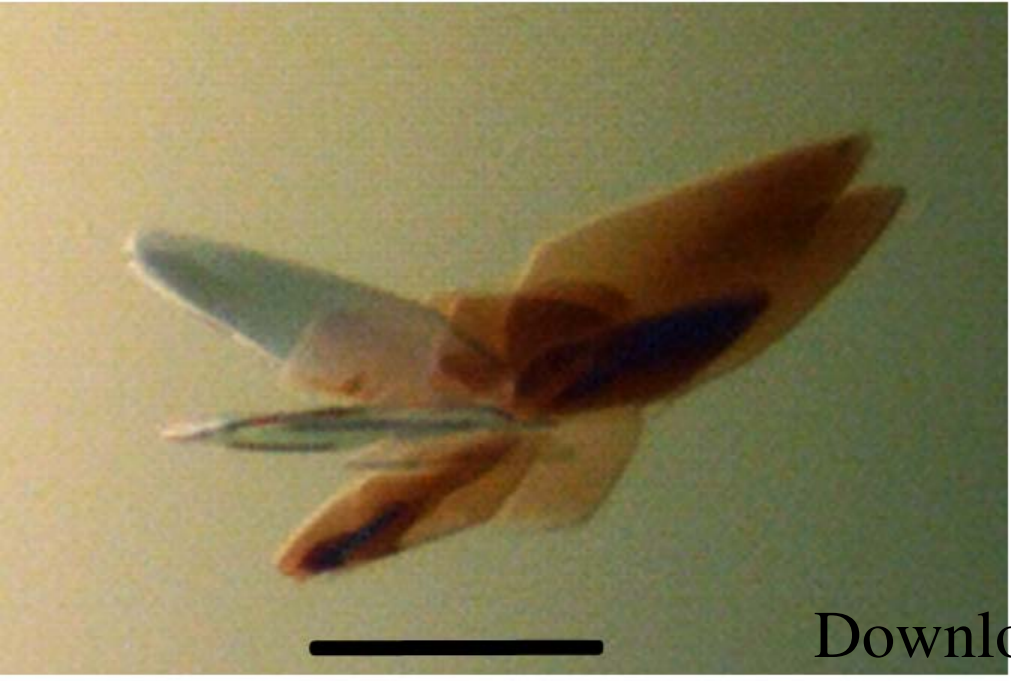

Figure 1

(a)

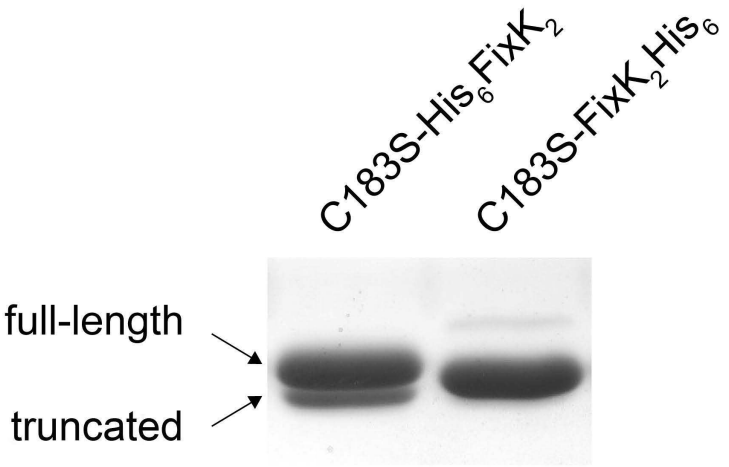
C183S-His6FixK2
C183S-FixK2His6
full-length
truncated

(b)

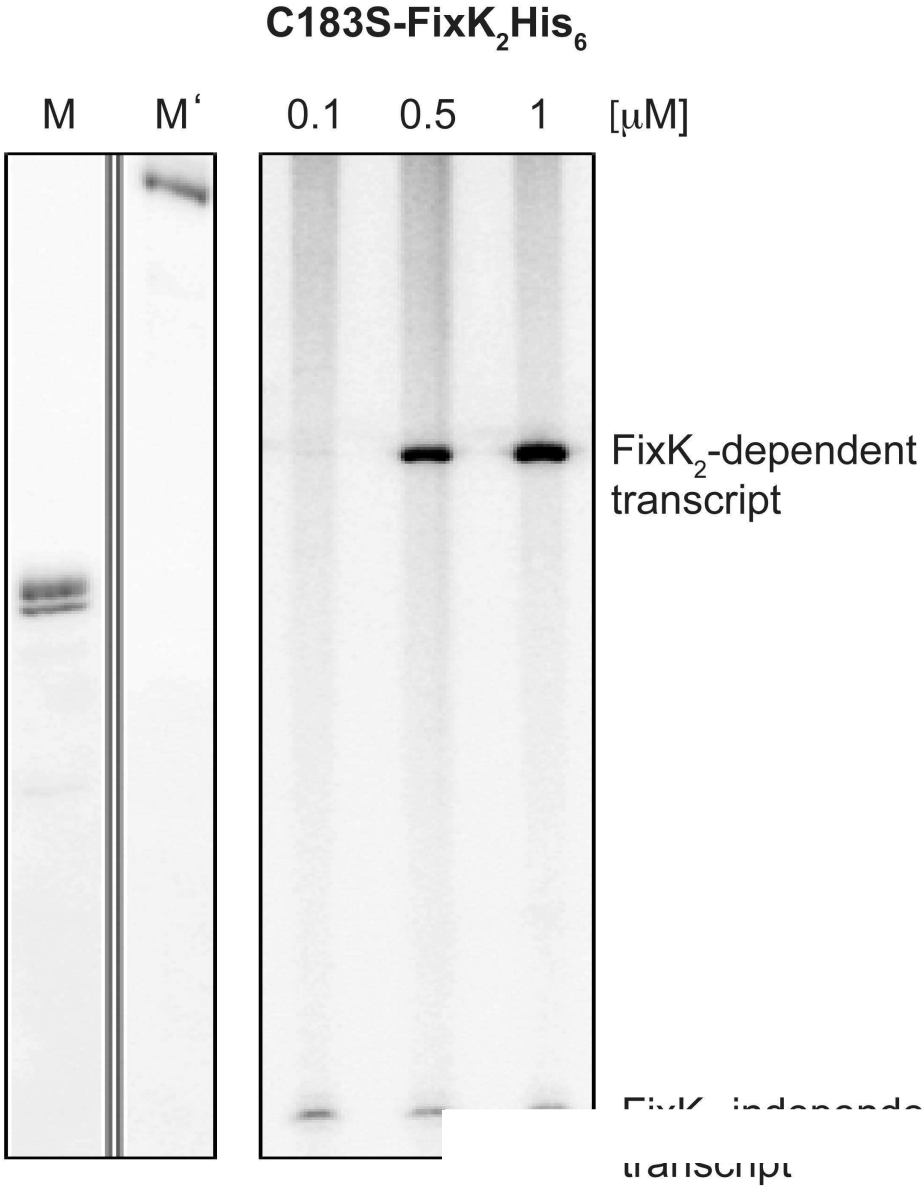
C183S-FixK2His6
M
M‘
0.1
0.5
1
[μM]
FixK2-dependent transcript
transcript

Figure 2

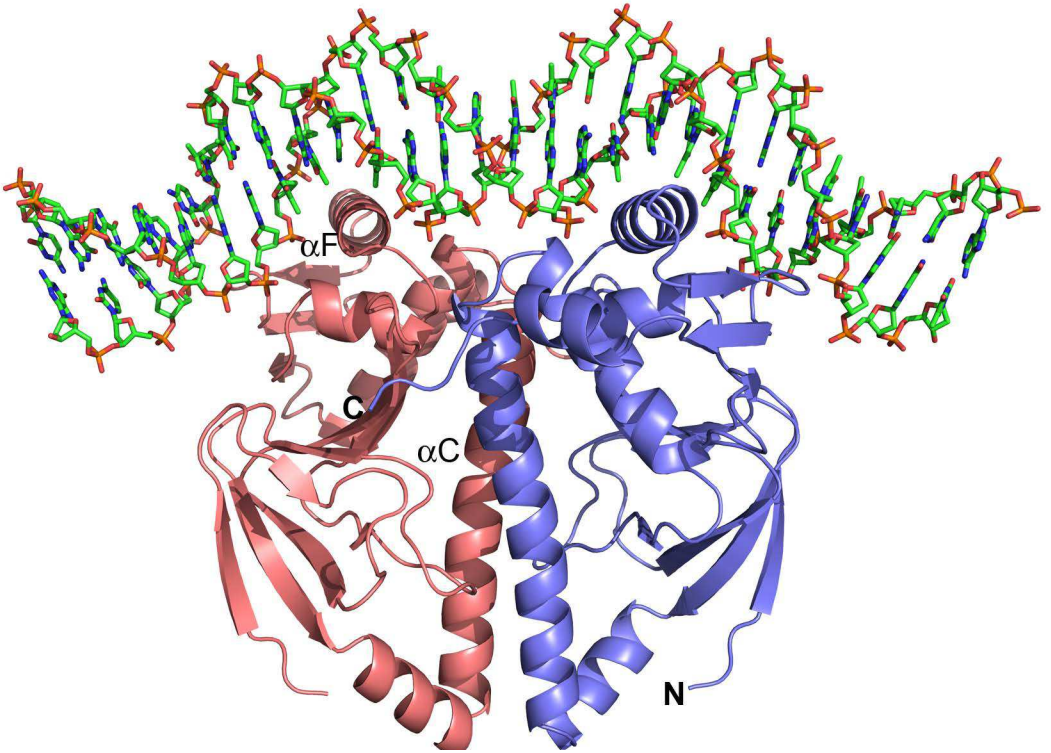

Figure 3

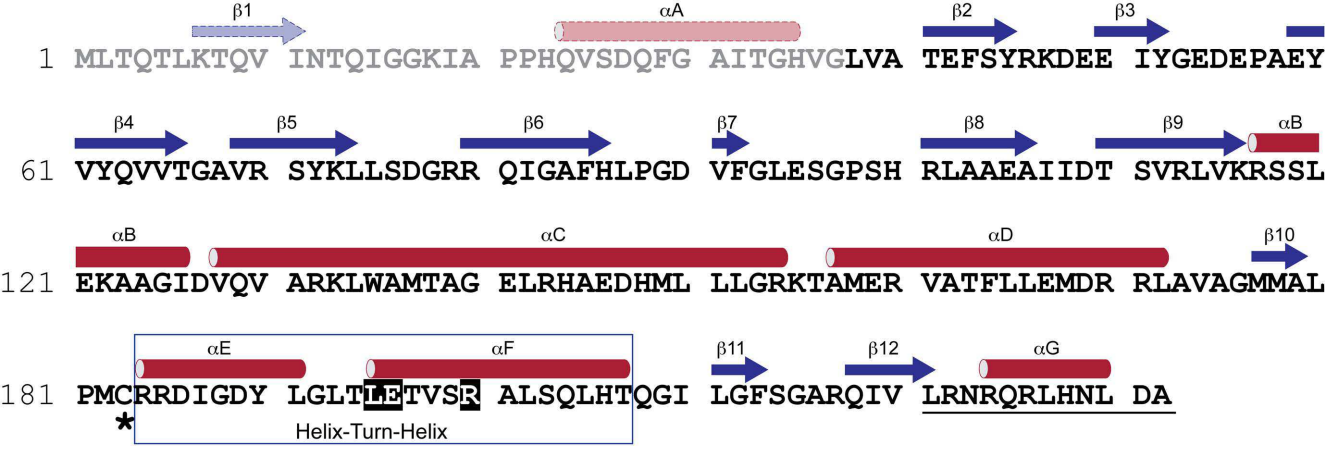
β1
αA
β2
β3
1 MLTQTLKTQV INTQIGGKIA PPHQVSDQFG AITGHVGLVA TEFSYRKDEE IYGEDEPAEY
β4
β5
β6
β7
β8
β9
αB
61 VYQVVTGAVR SYKLLSDGRR QIGAFHLPGD VFGLESGPSH RLAAEAIIDT SVRLVKRSSL
αB
αC
αD
β10
121 EKAAGIDVQV ARKLWAMTAG ELRHAEDHML LLGRKTAMER VATFLLEMDR RLAVAGMMAL
αE
αF
β11
β12
αG
181 PMCRRDIGDY LGLTLETVSR ALSQLHTQGI LGFSGARQIV LRNRQRLHNL DA
*
Helix-Turn-Helix

Figure 4

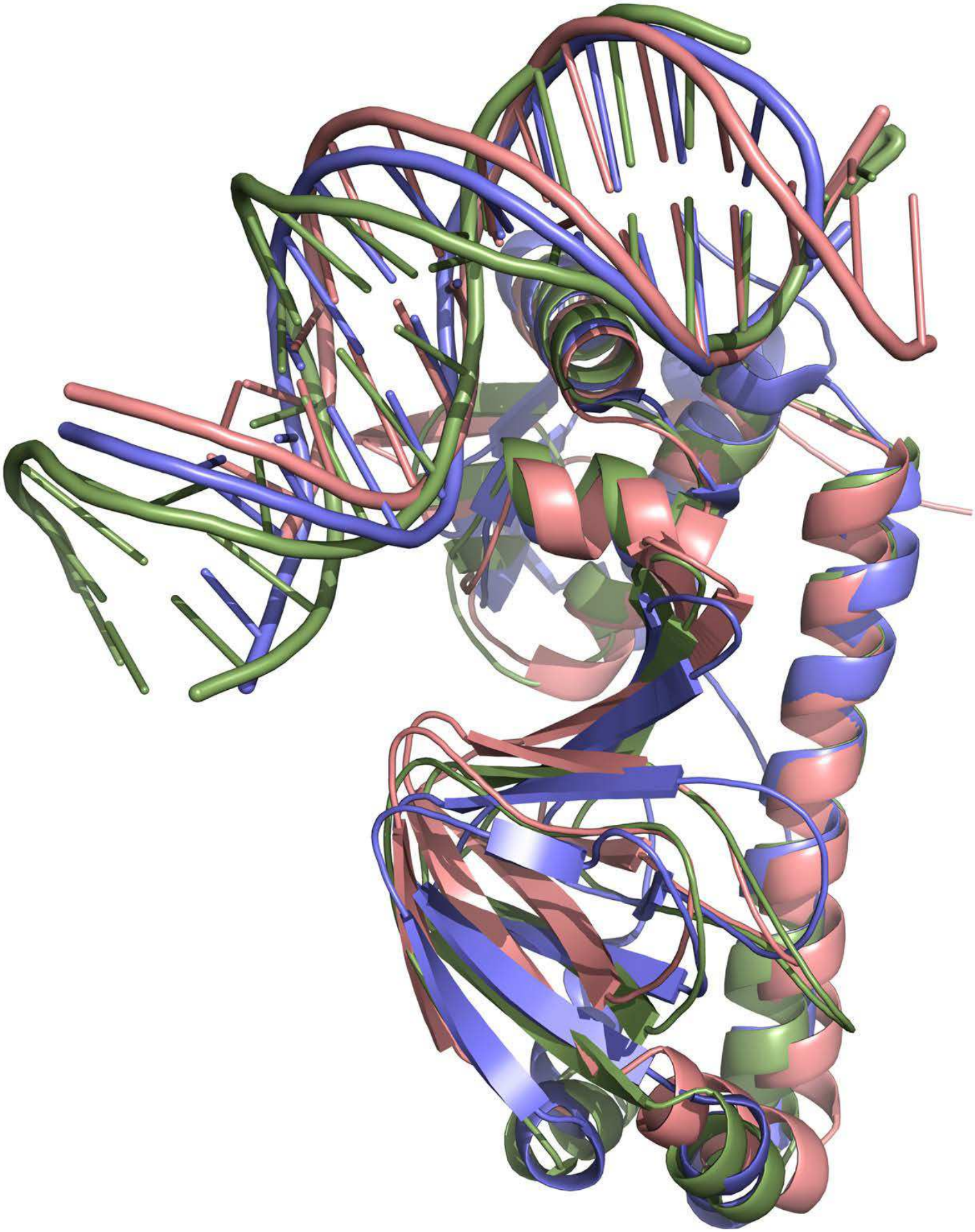

Figure 5

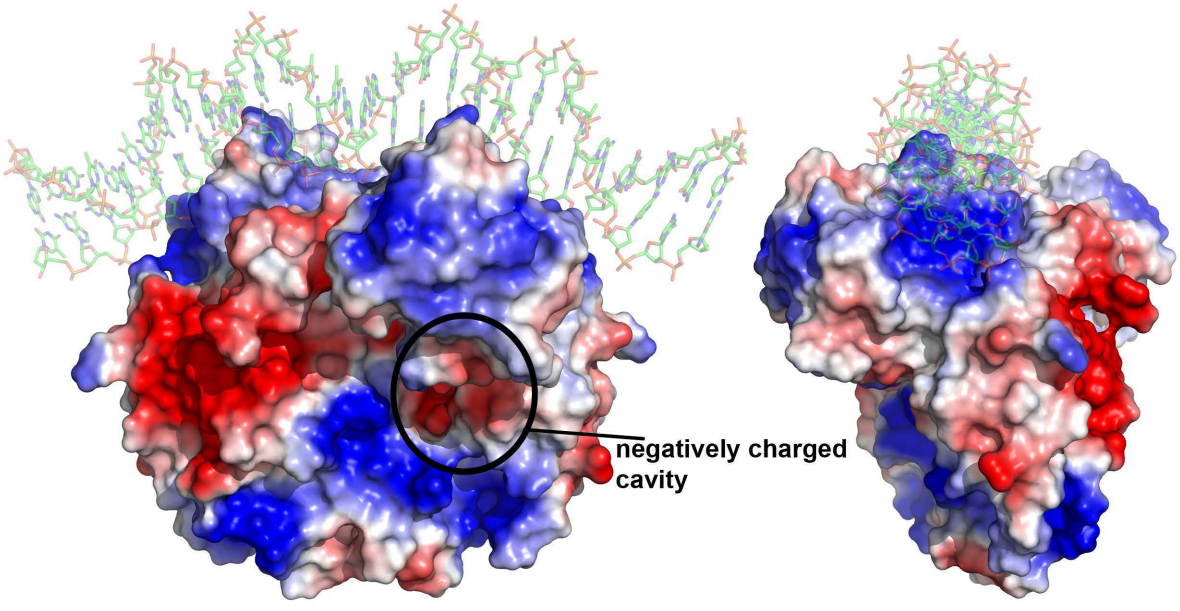

Figure 6

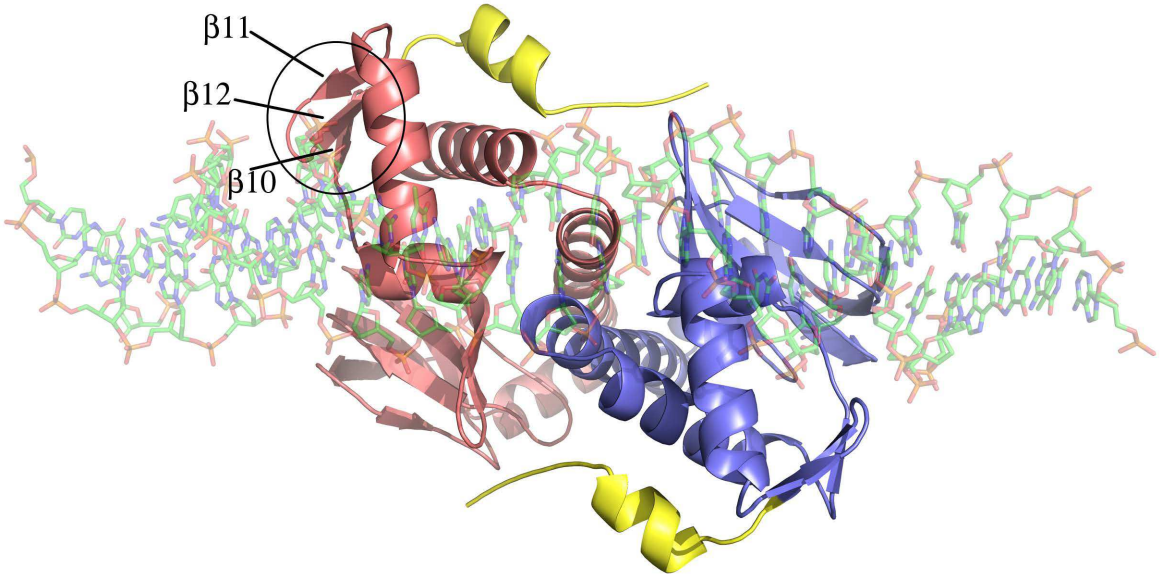

Figure 7

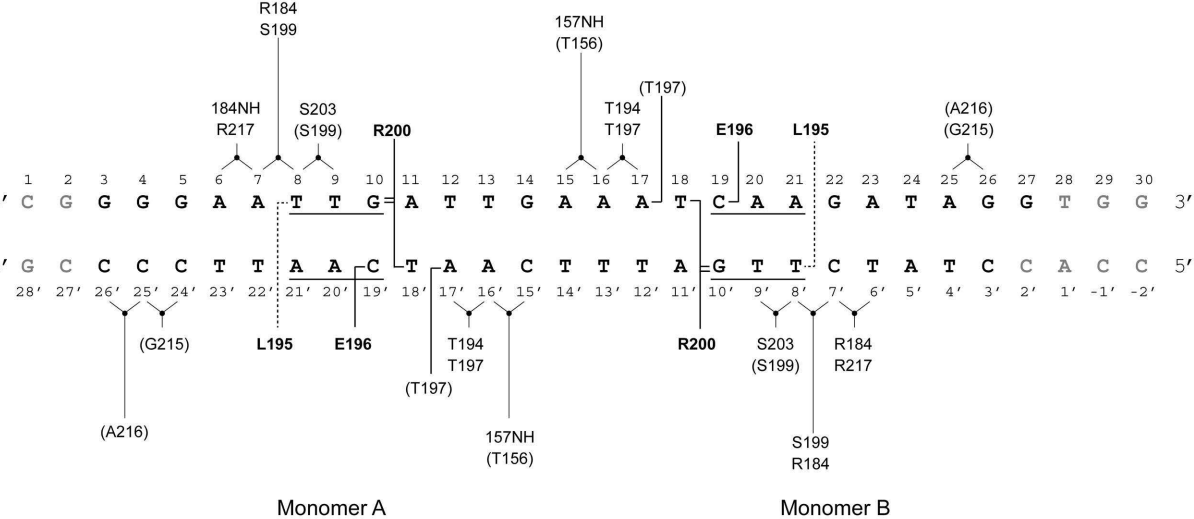

interaction with phosphate backbone

( ) interaction through water

------ hydrophobic interaction

Figure 8

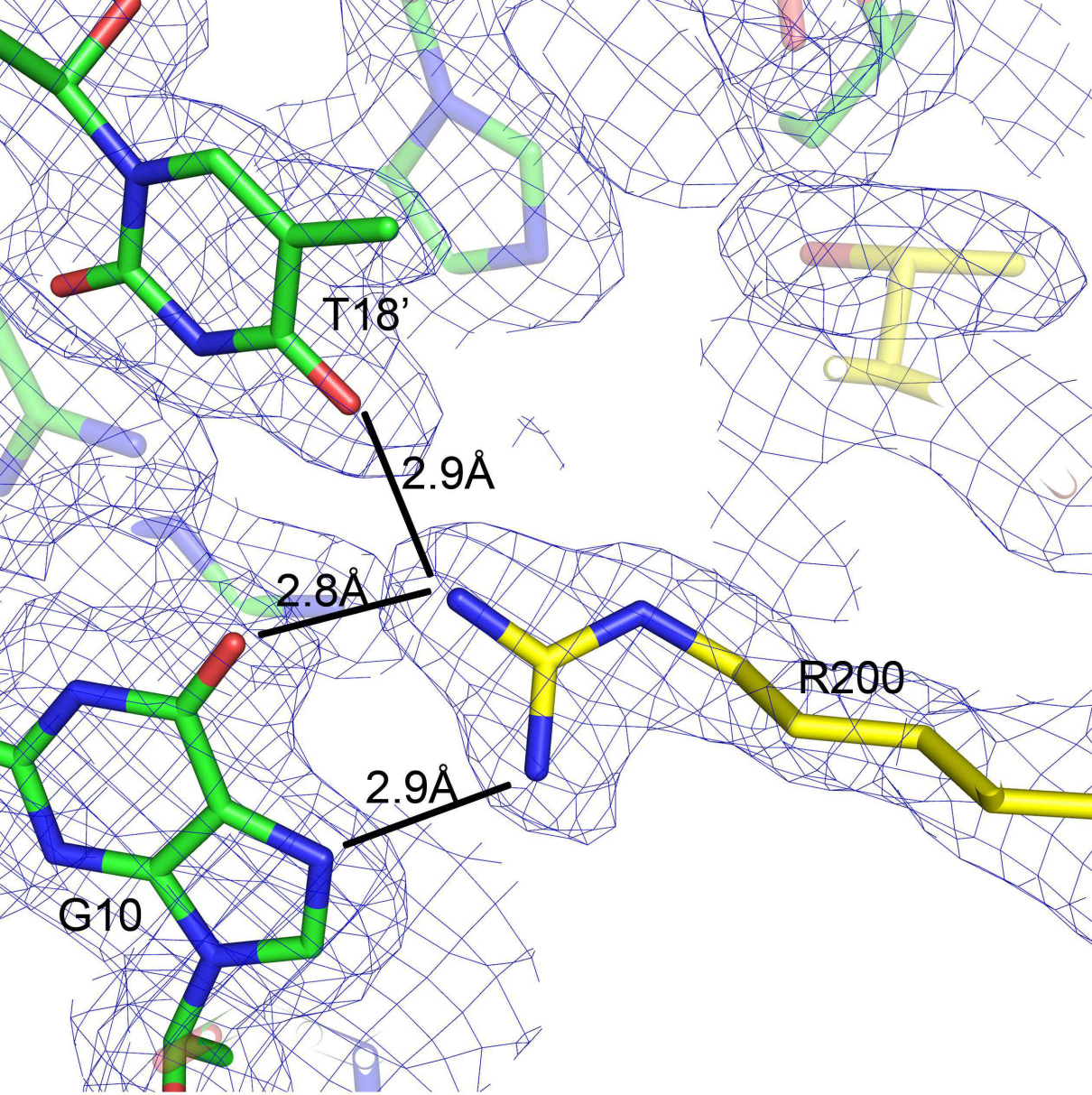

Figure 9

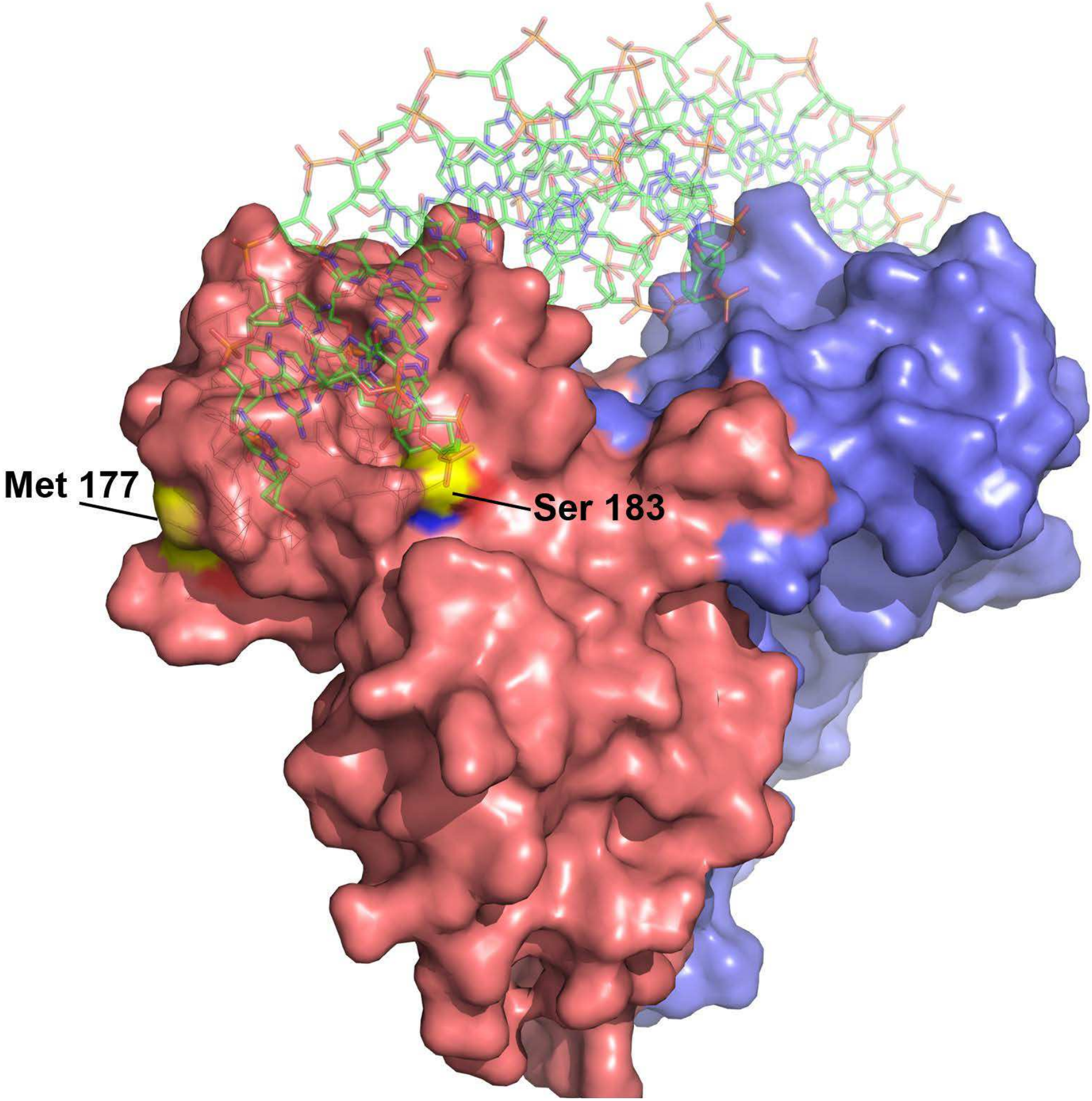

Figure 10

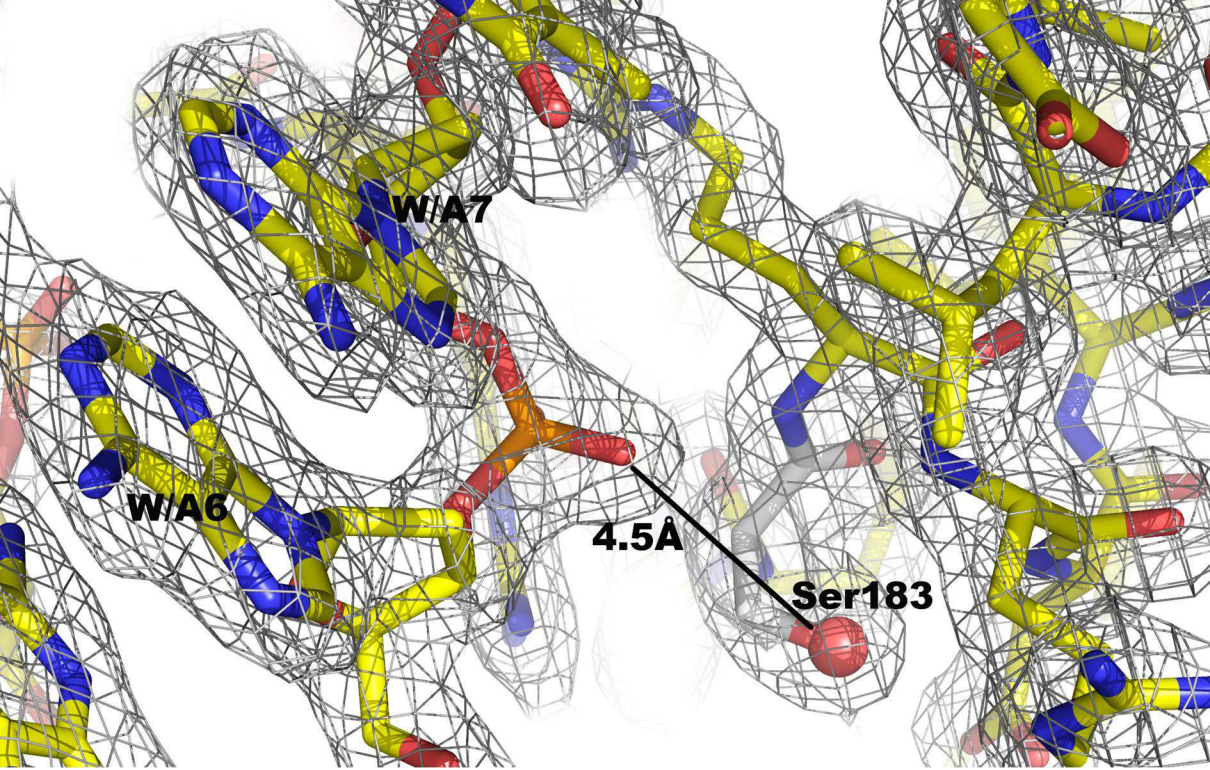

Figure 11